Maker fringes in the Terahertz radiation produced by a 2-color laser field in air

Yi Liu, Aurélien Houard, Magali Durand, Bernard Prade, André Mysyrowicz

Maker fringes in the Terahertz radiation produced by a 2-color laser field in air

Y. Liu, A. Houard, M. Durand, B. Prade, A. Mysyrowicz*

Laboratoire d'Optique Appliquée, ENSTA, Ecole Polytechnique, CNRS UMR 7639, Palaiseau, 91761, France
Corresponding author: andre.mysyrowicz@ensta.fr

Abstract: The terahertz radiation produced by a 2-color femtosecond laser scheme strongly saturates and develops an oscillatory behavior with increasing power of the driving femtosecond laser pulses. This is explained by the formation of a plasma channel due to filamentation. Due to dispersion inside the filament and the Gouy phase shift, the phase difference between the 800 nm and 400 nm pulses varies along this plasma emitter. As a result, the local THz radiations generated along the filament interfere destructively or constructively, which manifests itself in the form of Maker fringes.

OCIS codes: (190.7110) Ultrafast nonlinear optics; (300.6495) Spectroscopy, terahertz; (350.5400) Plasma; (260.5210) Photoionization.

References:

1. M. Kress, T. Löffler, S. Eden, M. Thomson, and H. G. Roskos, "Terahertz-pulse generation by photoionization of air with laser pulses composed of both fundamental and second-harmonic waves, " Opt. Lett. **29**, 1120-1122 (2004).
2. X. Xie, J. Dai, and X.-C. Zhang, "Coherent control of THz wave generation in ambient air," Phys. Rev. Lett. **96**, 075005 (2006).
3. K. Y. Kim, J. H. Glownia, A. J. Taylor, and G. Rodriguez, "Terahertz emission from ultrafast ionizing air in symmetry-broken laser fields," Opt. Express. **8**, 4577-4584 (2008).
4. A. Couairon and A. Mysyrowicz, "Femtosecond filamentation in transparent media," Phys. Rep. **441**, 47-189 (2007).
5. S. Tzortzakis, G. Méchain, G. -B. Patalano, Y. -B. André, M. Franco, B. Prade, A. Mysyrowicz, J. -M. Munier, M. Gheudin, G. Beaudin, P. Encrenaz, "Coherent sub-THz radiation from femtosecond infrared filaments in air," Opt. Lett. **27**, 1944-1946 (2002).
6. We also performed an independent experiment with properly chosen experimental parameters and carefully aligned BBO crystal to test how the THz yield depends on the BBO-focus distance. In these measurements, a sin-like dependence was confirmed for 3 largely different BBO rotation angle.
7. H. Zhong, N. Karpowicz, and X. -C. Zhang, "Terahertz emission profile from laser-induced air plasma," Appl. Phys. Lett. **88**, 261103-261105 (2006).
8. P. D. Maker, R. W. Terhune, M. Nisenoff, and C. M. Savage, "Effects of dispersion and focusing on the production of optical harmonic," Phys. Rev. Lett. **8**, 21-22 (1962).
9. A. Proulx, A. Talebpour, S. Petit, and S. L. Chin, "Fast pulsed electrical field created from the self-generated filament of a femtosecond Ti:sapphire laser pulse in air," Opt. Comm. **174**, 305-309 (2000).
10. S. A. Hosseini, B. Ferland, and S. L. Chin, "Measurement of filament length generated by an intense femtosecond laser pulse using electromagnetic radiation detection," Appl. Phys. B **76**, 583-586 (2003).
11. F. Lindner, G. G. Paulus, H. Walther, A. Baltuska, E. Goulielmakis, M. Lezius, and F. Krausz, "Gouy phase shift for a few-cycle laser pulse," Phy. Rev. Lett. **92**, 113001(2004).
12. H. R. Lange, A. Chiron, J. F. Ripoche, A. Mysyrowicz, P. Breger, and P. Agostini, "High-order harmonic generation and quasiphase matching in Xenon using self-guided femtosecond pulses," Phys. Rev. Lett. **81**, 1611-1664 (1998).

1. Introduction

Mixing of an 800nm femtosecond pulse with its phase-controlled second harmonic in partially ionized air is a very efficient technique for the generation of intense THz pulse [1-3]. For example, THz pulse of 5μJ can be routinely obtained with a table-top femtosecond laser

system [3]. Even more intense THz pulses can be expected by up-scaling the intensity of the femtosecond pulses since there is no optical element in the focus of the beams. This type of THz source has been proposed for stand-off THz applications because the poor transmission of a THz wave in ambient air could be overcome [2]. Up to now, most of the THz generation with this technique has been obtained with lasers of relatively modest power (< 10 GW) in a tightly focused geometry. In this case, the ionized region of air is limited to a length of a few millimeters, comparable to the Rayleigh distance of the beams. The theoretical modeling of the THz emission was therefore treated by considering a localized radiation source [1-3]. In order to scale up the THz energy, more powerful femtosecond pulses must be employed. For remote illumination with THz, it will also be necessary to use focusing elements of small numerical aperture to prevent local dielectric breakdown. Under such conditions, the formation of a long plasma filament is unavoidable [4]. To our knowledge, the effects of such an extended plasma on the THz generation efficiency have not yet been explored.

In this paper, we show that the THz energy exhibits an oscillating behavior with the scaling up of the IR laser intensity. Further experiments reveal that the local THz generated on both extremities of a long filament have opposite polarities, which leads to destructive interference in the far field. All these observations show that there is a serious intrinsic limitation of the two-color scheme for achieving THz emission at long range with high power.

2. Results and discussion

In the experiments, a commercial femtosecond laser system (Alpha-100, Thales) was used, which delivers 15 mJ pulses of 50 fs at a repetition rate of 100Hz. The pulses were focused by convex lenses of focal length 100, 300, 500, 750, and 1000mm in ambient air. Between the lens and the geometrical focus, a type-I BBO crystal of 100μm thickness was inserted in the beam. The THz generated by the air plasma was collimated by an off axis parabolic mirror of f = 120mm and sent to the detection system (Fig. 1(a)). The THz radiation was detected by a heterodyne THz detector, which is sensitive to the 0.1THz component of the THz radiation with a bandwidth of 4GHz [5].

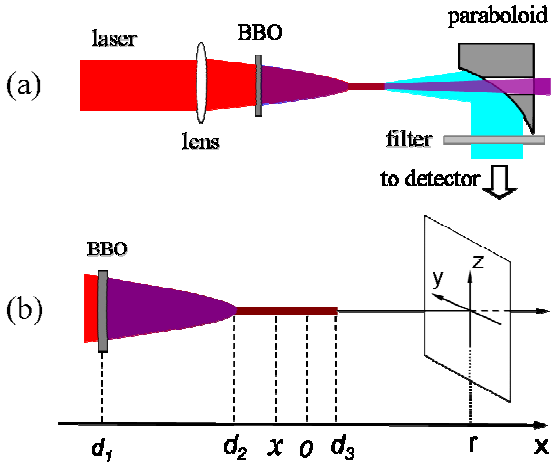

Fig. 1. (a) schematic experimental setup, (b) modeling of the filament THz emitter (see the text for details).

We first measured the THz intensity versus the IR energy E_{IR} using a lens of f = 500 mm. The result is presented in Fig. 2. An IR laser energy threshold of 150 μJ was observed, which corresponds to a laser intensity of 5×10^{13}W/cm^2 at the focus. This intensity corresponds to the onset of plasma formation by multiphoton ionization [1-3]. In such a measurement, the distance d between BBO and focal point matters because it fixes the relative phase between

the fields at ω and 2ω at the focus. In the limit of a localized plasma, the THz field amplitude varies like $E_{THz} \propto \sin(\Delta\varphi)$, where the phase difference $\Delta\varphi = \varphi_{400} - \varphi_{800} = \omega\left(n_{2\omega}^{air} - n_{\omega}^{air}\right)d/c$ is due to the dispersion of air [3, 6]. The distance d = 338 mm between the BBO crystal and the focal point was set such that it optimizes the THz output for an energy E_{IR} = 165 μJ close to the threshold for THz appearance. An oscillatory behavior of the THz intensity was observed when the laser pulse energy E_{IR} was increased. A similar phenomenon was found with all lenses mentioned above. This observation is distinct from several previous reports, where the THz increases monotonously with the scaling up of the IR energy (although a saturation was observed at high energies in reference 3).

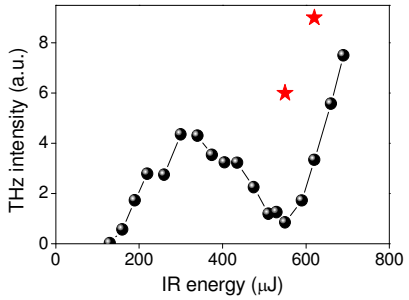

Fig. 2. Terahertz intensity as a function of the incident IR pulse energy. The stars show the results with the BK7 rephaser for quasi phase matching.

To get insight on the origin of this oscillatory phenomenon, we inspected more closely the plasma emitter. In Fig. 3(a), (c), and (e), the fluorescence images of the filaments for typical input energy are presented. The blue tracks correspond to the emission from ionized air molecules. They yield directly the length of the plasma channel produced during filamentation. For E_{IR} = 210, 340, and 510 μJ, the length of the filament is determined to be 11, 18, and 25mm, respectively.

As mentioned above, tightly focused beams were employed in most previous studies [1-3], so that the plasma filaments were less than a few millimeters in length. In such a case, the local THz generated along the short plasma channel adds up constructively [7]. To check the contribution of each local THz emitters along the **extended** filament in the far field, a circular metallic aperture with a 1 mm hole at the center was mounted around the filament. The outer diameter of this metallic blocker was 20 mm. This aperture blocked the THz generated by the filament segment behind it, but it did not disturb the filament formation and the THz generation in front of it. In the experiments, the aperture was scanned along the filament axis. The resulting THz intensity is presented in Fig. 3(b), (d), and (f) for different IR laser pulse energies corresponding to Fig. 3(a), (c), and (e). For E_{IR} = 210 μJ, the THz intensity decreases monotonously and eventually reaches zero when the aperture blocks the terahertz generating segment entirely. This agrees with previous similar observations by H. Zhong *et al* [7]. However, for E_{IR} = 510 μJ, where the THz yield is a minimum without the aperture, it is found that the THz intensity starts to **increase** when the aperture moves downstream the filament. After reaching a maximum, the THz intensity decreases gradually to zero. For an incident energy of 340 μJ, between the above two cases, an intermediate behavior was observed. These observations show that the local THz emission develops opposite polarities for increasing filament length, which interfere destructively in the far field. This is a manifestation of the well-known Maker fringes for this down conversion process [8].

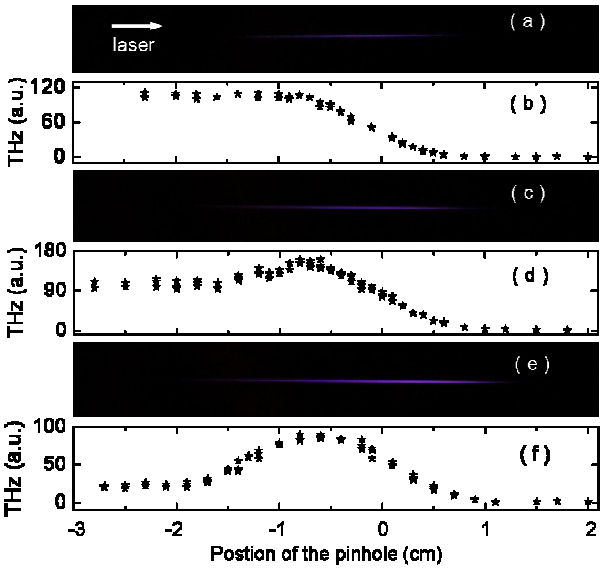

Fig. 3. Luminescence images of the filaments for IR input energy of (a) 210 μJ, (c) 340 μJ, (e) 510 μJ. In (b), (d), (f), the THz intensity are plotted as function of the position of the scanning aperture. The aperture is scanned from left to right. In (b), the local emitters along the filament interfere constructively in the far field, while in (f) they interfere destructively.

To detect the electric properties of the local emitter along the filament, we employed an electromagnetic wave antenna [9, 10]. A needle-shaped antenna was connected by a SMA cable to a 1 GHz oscilloscope having a 50 Ohm impedance. In the experiments, the antenna was 3 mm away from the filament. As shown in Fig. 4(a) and (b), the detected signal has a duration of 1 ns which is the limit of our oscilloscope. In a first experiment, the antenna was fixed at the starting segment of a long filament. The peak-to-peak amplitude of the detected field exhibits an oscillatory behavior when the BBO-focus distance is changed continually, as plotted in Fig. 4(c). The signal was observed to oscillate with a period of 55 mm. It is well known that the amplitude of the THz field exhibits an oscillatory behavior when the BBO-focus distance is changed continually (see Fig. 2 of reference 1), which is due to the periodic phase-shift between the 400 nm and 800 nm pulses induced by air dispersion [1, 3]. The

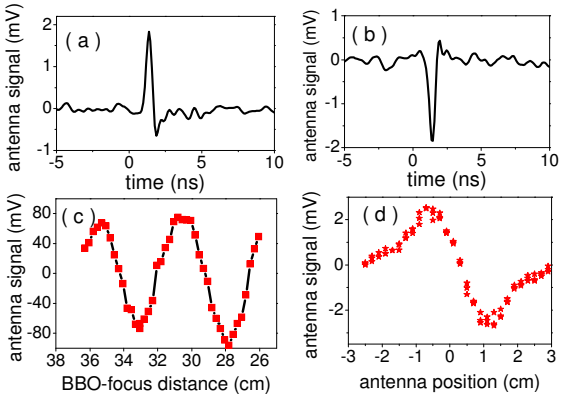

Fig. 4. (a) and (b) typical antenna signals with opposite polarities. (c) Peak-to-peak amplitude of the antenna signal as a function of the BBO to geometric focus distance. The focal lens is 1000 mm and the antenna is positioned at the beginning of the filament. (d) Peak-to-peak amplitude of the antenna signal along the filament shown in Fig. 3(e). This polarity reversal could be closely related to the Gouy phase shift [11] and will be discussed in more detail at the end of this paper.

identical observations in Fig. 4(c) with that of Fig. 2 in ref. 1 therefore suggests that the polarity of the antenna signal reflects the phase difference between the 800nm pulse and its second harmonic. In a second experiment, in the same condition as those of Fig. 2(e) the antenna was scanned along the filament. The signal amplitude is presented in Fig. 4(d). We found that the signals detected at the leading and trailing parts of the filament show different polarities, which confirms our analysis of the previous paragraph.

In the above experiments the BBO crystal was fixed at the position d = 338 mm, which is optimized for E_{IR} = 165 μJ. To check the role of the phase difference $\Delta\varphi$ induced by air in the case of a long filament, we have measured the THz output as a function of BBO-focus distance for different incident IR energies. The results for f = 500 mm are presented in Fig. 5(a). Two features are noticed. First, periodic oscillations are observed for all incident energies. Here, the period of 27.5 mm is half of that obtained when the amplitude is measured [1] because we measured the THz intensity instead of the THz amplitude. Second, we observed that the optimal position for THz generation shifted gradually upstream with the increase of E_{IR}. For instance, the oscillation curve moves by almost half a cycle when the laser energy is increased from 165 μJ to 510 μJ. As a result, when the BBO is fixed at position A (d = 338 mm), the THz intensity is on the verge of an ascending oscillation behavior with increasing IR energy. This explains the phenomenon presented in Fig. 2.

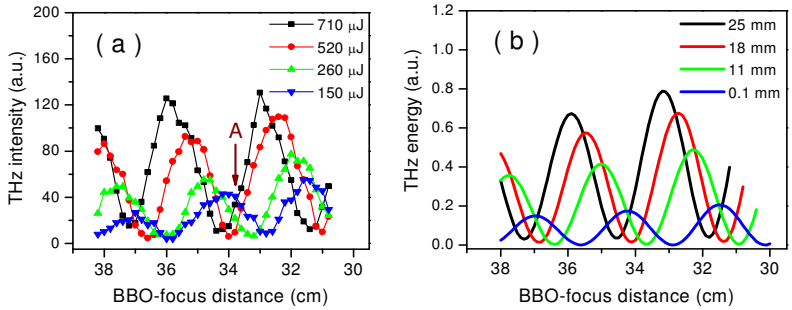

Fig. 5. THz signal as a function of the BBO to geometric focus distance. (a) experimental results. For comparison, the signals in the case of 150 μJ and 260 μJ have been multiplied by factor of 20 and 4, respectively. (b) calculated results. The THz energy is obtained at r = 12cm by integration for a detector radius of 2cm. The THz energy for the emitters with different length are not to the same scale.

Why does the optimal position for THz generation change with IR laser pulse energy? In our present case, the filament is significantly longer than the THz wavelength. Therefore, the phase variation of the 800nm and 400nm pulses along the extended filament cannot be neglected. Inside the filament, the contribution to the refractive index due to the defocusing plasma is $-\rho/2\rho_c$, where $\rho_c = \varepsilon_0 m\omega^2/e^2$ is the plasma frequency. Also, the Kerr effect and cross phase modulation effect change the index of 800 nm and 400 nm by $n_2 I_{800}$ and $n_2^{'} I_{800}$, where $n_2 = 3\times10^{-19}\, W/cm^2$ and $n_2^{'} = n_2/3$ are the corresponding nonlinear coefficients [4]. In addition, the Gouy phase shift of 400 nm and 800 nm pulses can also induce a phase difference [11]. A full theoretical consideration of the dispersion inside the filament requires labor-consuming numerical simulations of the propagation process to obtain the plasma density and laser intensity for each input power. Here, we simply simulate the filament as a uniform one dimension line source (see Fig. 1(b)) due to the fact that the laser intensity and plasma density are quite constant inside the filament [4]. The origin of the axis was chosen at the geometrical focus of the laser beam. The positions of the BBO crystal, the starting point and the end of the filament are denoted by d_1, d_2, and d_3, respectively. Therefore, the phase difference between the 400 nm and 800 nm pulses at position x is obtained as

$$\Delta\varphi(x) = \omega(n_{2\omega}^{a} - n_{\omega}^{a})(d_2 - d_1) + \omega(n_{2\omega}^{p} - n_{\omega}^{p})(x - d_2) + \left(-\arctan\left(x/z_R^{400}\right) + \arctan\left(x/z_R^{800}\right)\right)$$

The first and second terms denote the dispersion in air and filament plasma, where $n_{2\omega}^{a}, n_{\omega}^{a}, n_{2\omega}^{p}, n_{\omega}^{p}$ are the refractive index of 400 nm and 800 nm pulses in air and plasma, respectively. The third term presents the phase difference due to the Gouy phase shift, where the z_R^{400} and z_R^{800} are the Rayleigh lengths of the two pulses. As a result, the THz field at position (*r, y, z*) in the far field can be expressed as:

$$THz(r,y,z) = \int_{d_2}^{d_3} \frac{THz(x)}{\sqrt{(r-x)^2 + y^2 + z^2}} \exp\left[-i\left(k_{THz}\sqrt{(r-x)^2 + y^2 + z^2} - \omega_{THz}\frac{x}{c}\right)\right]dx$$

$$\approx \frac{1}{r}\int_{d_2}^{d_3} \sin[\Delta\varphi(x)]\exp(i\Delta\varphi(x))\exp\left[-i\left(k_{THz}\sqrt{(r-x)^2 + y^2 + z^2} - \omega_{THz}\frac{x}{c}\right)\right]dx$$

The term $\exp(i\Delta\varphi(x))$ takes into account the different initial phase of the local THz emitter [2]. Fig. 5(b) and (c) present the calculated results at r = 12cm for a detector dimension of $\rho = \sqrt{y^2 + z^2} = 2cm$. In the simulations, the unknown dispersion inside filament $n_{2\omega}^{p} - n_{\omega}^{p}$ was used as a fitting parameter and the position-dependent conversion of 2ω generation were also taken into account. We found that in the case of $n_{2\omega}^{p} - n_{\omega}^{p} = 0.3(n_{2\omega}^{a} - n_{\omega}^{a})$, the theoretical results in Fig. 5(b) agree qualitatively with the experimental observations in Fig. 5(a) if we adopted the following values for the laser intensity and plasma density in the filament: I = 3.9×10^{13}W/cm^2 and $\rho = 10^{16}$cm^{-3}. These values are consistent with the previous estimations [4].

The polarity reversal of the antenna signal has been observed in Fig. 4(d) due to the Gouy phase shift and the dispersion of the 800 nm and 400 nm pulses. Like in the quasi-phase matching technique implemented for harmonic generation in filament [12], the THz yield should be enhanced if a phase reversal between 800nm and 400nm is achieved at the turning point of Fig. 3(f). To verify this point, we employed a 170 μm BK7 cover plate as a rephaser, which was found to be transparent at 0.1 THz. The results obtained with a properly positioned rephaser are presented in Fig. 2. The THz intensity was found to be 6 times higher than that without the platelet in the case of E_{IR} = 510 μJ. Damage appeared on the cover plate a few seconds after the onset of irradiation and renovation to a fresh area was necessary. This limits the use of this rephaser as a practical way to achieve more overall conversion into THz radiation.

3. Conclusion

In conclusion, the local THz emitters along a long plasma filament possess different polarities which can lead to destructive interference at far field. This intrinsic limitation lowers the conversion efficiency of this 2-color laser field method for THz generation with an extended plasma filament, posing an inherent obstacle for the stand-off THz generation and related applications. Inside the filament, a reduced dispersion is confirmed by comparing the experiment results and a theoretical calculation. Finally, in a proof of principle experiment a quasi-phase matching technique was demonstrated.